ORIGINAL PAPER

Electrochemiluminescence sensor based on methionine-modified gold nanoclusters for highly sensitive determination of dopamine released by cells

Huaping Peng[1,2] · Haohua Deng[1,2] · Meili Jian[1,2] · Ailin Liu[1,2] ·
Fengqiao Bai[1,2] · Xinhua Lin[1,2] · Wei Chen[1,2] (iD)

Abstract The electrogenerated chemiluminescence (ECL) of methionine stabilized gold nanoclusters (Met-AuNCs) is presented. The Met-AuNCs were used to modify a glassy carbon electrode (Met-AuNC/GCE) which is shown to exhibit a stable and strong cathodic ECL signal (at −1.86 V) when using potassium peroxodisulfate ($K_2S_2O_8$) as the coreactant in aqueous solution of pH 7.4. Compared to a GCE modified with BSA-AuNCs, the ECL intensity of Met-AuNCs is 5-fold enhanced. The possible ECL reaction mechanism of the ECL system was studied, and a method for the determination of dopamine (DA) was worked out. The modified GCE has a linear response in the 0.1 to 4 μM DA concentration range, with a detection limit of 32 nM (at an S/N ratio of 3). The method was applied to the determination of DA released by PC12 cells. In our perception, the Met-AuNC/GCE provides a viable new tool in ECL based bioanalysis that also paves new routes to the design and application of new sensors.

Huaping Peng and Haohua Deng contributed equally to this work

✉ Wei Chen
chenandhu@163.com

1 Department of Pharmaceutical Analysis, Fujian Medical University, Fuzhou 350122, China

2 Higher Educational Key Laboratory for Nano Biomedical Technology of Fujian Province, Fujian Medical University, Fuzhou 350122, China

Introduction

Electrochemiluminescence (ECL) represents a marriage between electrochemistry and spectroscopy. Since it does not require the use of an external light source, problems derived by light scattering in spectroscopic-based techniques are avoided, improving the signal-to-noise ratio dramatically. In addition, the time and position of light-emitting reactions can be accurately controlled by the potential applied at an electrode surface. Due to its simplicity, rapidity, excellent detection sensitivity, high selectivity, easy controllability and flexibility, ECL detection has emerged as a powerful tool in analytical chemistry related areas such as medical diagnostics, environmental and food monitoring, and biowarfare agent detection [1–4].

One of the key tasks of ECL research is to identify new luminophore species. Quantum dots (QDs) have been extensively used in ECL-based detection [3, 5, 6]. Compared with conventional molecular emitters, QDs own several distinctive merits like size/surface-trap controlled luminescence and good stability against photobleaching. However, up to now, most QDs used as luminophore species are toxic heavy metals-based semiconductors, such as CdSe, CdS, and PbS. Obviously, the intrinsic toxicity of these QDs would limit their applications in ECL sensors, especially in bioanalysis. Therefore, it is of considerable interest in developing environment-friendly ECL luminophores for biosensing. To explore novel "green" luminophores with high ECL

efficiency, the family of nanoemitters has been enlarged from exclusively QDs to other miscellaneous nanomaterials with various compositions, sizes and shapes, such as Ag_2Se QDs [7], carbon nanodots [8], Ag-carbon nanodots [9], and graphene QDs [10]. Emerging as a novel type of nontoxic and harmless luminescent nanomaterial, gold nanoclusters (AuNCs) have drawn wide attention [11–16]. Their size falls within the range of the Fermi wavelength of conduction electrons and results in size-dependent HOMO–LUMO transition and luminescence. Furthermore, AuNCs show fantastic characteristics including remarkable water-solubility, high colloidal stability, outstanding catalytic performance, and unusual photophysical properties, which make them promising in biosensing and labeling applications [17–23]. Although the fluorescent properties of AuNCs have been widely studied, there are only a few researches about the AuNC-based ECL sensing, even less in aqueous system and by using immobilization mode [24, 25].

Herein, we reported of the ECL property of methionine stabilized AuNCs (Met-AuNCs). The Met-AuNCs were synthesized by using methionine both as a reductant and a stabilizer, and the ECL properties of the Met-AuNC-modified glassy carbon electrode (Met-AuNC/GCE) were studied. The excellent cathodic ECL behavior has been observed with $K_2S_2O_8$ as coreactant and the ECL mechanism has been discussed. Moreover, dopamine (DA) was taken as a model analyte to evaluate the potential application of the Met-AuNC-based ECL sensor. The practicality of the Met-AuNC/GCE was validated by determining the DA released from PC12 cells via exocytosis through stimulation of potassium ions. This ECL sensor is environmental friendly, highly selective and sensitive, which can be widely applied in biological analysis. In particular, this approach would open new routes to apply other NCs ECL in different aspects of biochemistry.

Materials and methods

Materials

$HAuCl_4·4H_2O$, methionine, and $NH_3·H_2O$ were purchased from Aladdin Reagent Company (https://www.sigmaaldrich.com). Dopamine was obtained from Alfa Aesar (http://alfaaesar.lookchem.com/). PC12 cells were purchased from Beijing DingGuo ChangSheng Biotechnology Co. Ltd. (http://www.dlcs100.com/). Phosphate buffer (PB, 0.2 M) with different pH were prepared by changing the ratio of Na_2HPO_4 and NaH_2PO_4. All other regents were of analytical grade and used as received without further purification. All solutions were prepared with ultrapure water. PB with elevated K^+ included 104.2 mM KCl, 50 mM NaCl, 2 mM $CaCl_2$, 0.7 mM $MgCl_2$, 1 mM NaH_2PO_4, and 10 mM HEPES. Culture media and all the solutions were

adjusted to pH 7.4 by adding the appropriate volumes of 1 M NaOH.

Apparatus

Cyclic voltammetric (CV) and ECL measurements were obtained using a model MPI-A electro-chemiluminescence analyzer (Xi'an Remex Analysis Instrument Co. Ltd. Xi'an, China). The ECL spectra were obtained by collecting the ECL data during the cyclic potential sweep with a series of optical filters at wavelengths of 425, 440, 460, 490, 520, 535, 555, 575, 590, and 620 nm. The photoluminescence spectrum was measured by Cary Eclipse fluorescence spectrophotometer (Agilent, USA). The transmission electron microscope (TEM) was performed on JEOL 2010 transmission electron microscopy operated at an accelerating voltage of 200 kV.

Synthesis of Met-AuNCs

The Met-AuNCs were prepared according to our previous method [26]. Briefly, 4 mL of 0.1 M methionine and 0.6 mL of 0.5 M NaOH were added into 0.4 mL of 20 mg mL^{-1} $HAuCl_4$. The mixture solution was incubated at 37 °C for 6 h. Then, 0.5 mL of 1 M H_2SO_4 was added into the mixture to precipitate AuNCs. The product was collected with centrifugation at 6000 rpm (or with relative centrifugal force of 1815×g) for 2 min. Then the AuNCs were dissolved in a solution of $NH_3·H_2O$ (1.4%) and incubated at 70 °C for 30 min. The resulting solution of Met-AuNCs was stored in the dark at 4 °C.

Fabrication of the AuNC-modified GCE

Prior to use, the GCE was polished sequentially with 1.0, 0.3, and 0.05 μm alumina slurry, followed by washing thoroughly with water. Then, the electrode was washed ultrasonically with HNO_3, ethanol, and water, respectively. 100 μL of Met-AuNCs was mixed with 20 μL nafion (1.5%). 8 μL of the mixture was dropped on the GCE surface (3 mm in diameter, the surface area of the electrode is 0.0707 cm^2). After being dried in air at room temperature, the Met-AuNC-modified GCEs were obtained. For comparison experiments, the BSA-AuNCs were prepared (see the Supplemental data), and the final concentration of the BSA-AuNCs was the same as the Met-AuNCs. The BSA-AuNC-modified GCEs were prepared by the same procedure. To prepare the polydopamine (PDA)/Met-AuNC/GCE, 5 mg DA was dissolved in 1 mL of 5 mM Tris-HCl solution (pH 8.5), then Met-AuNC/GCE was immersed in it and stored in the 4 °C refrigerator for 2 h. Finally, the obtained PDA/Met-AuNC/GCE was washed by ultrapure water and stored in the 4 °C when not used.

Procedures

The ECL detection was performed at room temperature in the electrolyte containing $K_2S_2O_8$. The conventional three-electrode system was used through detection. A modified GCE was used as the working electrode, while a Pt wire as the auxiliary electrode, and an Ag/AgCl (saturated with KCl) electrode as the reference electrode. The potential was cycled between 0 and −2.0 V with a scan rate of 100 mV·s^{-1}, and the photomultiplier tube (PMT) was biased at 800 V in the experiments.

K$^+$-stimulated DA release from PC12 cells

The details of PC12 cell culture method were described as follows. PC12 cells were maintained in RPMI-1640 media supplemented with 10% fetal bovine serum (FBS), and 0.5% penicillin-streptomycin solution in a humidified atmosphere with 5% CO_2 at 37 °C. The medium was replaced every day throughout the lifetime of all cultures. ECL was applied to detect the K$^+$-stimulated release of DA from PC 12 cells [27]. Briefly, 0.5 mL of trypsin was added into the culture dishes for 1 min, and the PC12 cells in the culture dishes were suspended by culture medium. After that, the PC12 cells suspension on the culture dishes was centrifuged for 5 min at 1000 rpm, and washed 3 times with PB. Then, 5 mL of the elevated-K$^+$ PB were placed in the culture dishes (5×10^5 cells mL^{-1}), and incubated in the incubator for 10 min. After centrifuged, the supernatant was collected, and the extracellular fluids were transferred to sterilized beakers. Finally, the concentrations of DA in the mixtures with 0.1 M $K_2S_2O_8$ were determined by ECL.

Results and discussion

Choice of materials

Herein, to explore the ECL properties of the Met-AuNCs, different electrodes, such as Au electrode, Pt electrode, GCE and ITO electrode and different co-reactants such as H_2O_2, benzoyl peroxide (BPO), tri-npropylamine (TPrA) and $K_2S_2O_8$ were investigated. The results indicated that the Met-AuNC-modified GCE with $K_2S_2O_8$ as co-reactant in aqueous solution exhibited the most stable and efficient cathodic ECL signal. Therefore, GCE was used as the working electrode, and $S_2O_8{}^{2-}$ was chosen as the co-reactant to study the ECL properties of the Met-AuNCs.

Characterization of the Met-AuNCs

Transmission electron microscopy (TEM) revealed an average diameter of 2.5 ± ss0.3 nm for the Met-AuNCs (Fig. 1a). The inset high-resolution TEM image shows lattice planes separated by 0.236 nm, corresponding to the (111) lattice spacing of face-centered cubic Au [28]. The aqueous AuNCs solution emitted strong yellow fluorescence under UV light irradiation. By fluorescence spectrophotometry (excited at 420 nm), it was observed that the Met-AuNCs solution exhibited strong photoluminescence (PL) at around 535 nm (Fig. 1b). These phenomena corresponded to our previous results, indicating the successfully synthesized the Met-AuNCs [26].

ECL behaviors of Met-AuNC-modified GCE

ECL is a useful technique for both fundamental study and analytical applications. It is of considerable interest in exploring the ECL properties of the Met-AuNCs with excellent water-solubility. ECL behaviors of Met-AuNCs at GCE were investigated with cathodic coreactant $K_2S_2O_8$. Figure 2a shows the ECL curves on bare GCE and Met-AuNC/GCE at a scan rate of 100 mV·s^{-1} within the potential range of 0 to −2.0 V. Weak ECL emission can be observed on Met-AuNC/GCE in the absence of $K_2S_2O_8$ (Fig. 2a, curve a). After the addition of 0.1 M $K_2S_2O_8$, a strong ECL signal was obtained with the peak potential of −1.86 V (Fig. 2a, curve b). The CVs were also recorded simultaneously (Fig. S2). The cathodic peak at −1.0 V on Met-AuNC/GCE was corresponding to the reduction of $S_2O_8{}^{2-}$ [24, 29]. To gain a better

Fig. 1 a TEM image of Met-AuNCs. b Photoluminescence excitation (emission at 535 nm) and emission (excitation at 420 nm) spectra of Met-AuNCs
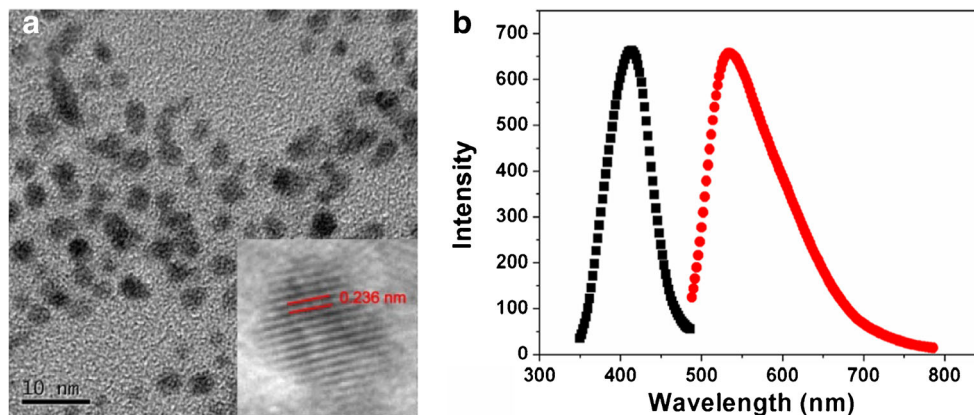
Fig. 2 a ECL intensity versus potential. (a) On the Met-AuNC/GCE in 0.2 M PB (pH 7.4) containing 0.1 M KCl; (b) on the Met-AuNC/GCE in 0.2 M PB (pH 7.4) containing 0.1 M $K_2S_2O_8$ and 0.1 M KCl; (c) on the bare GCE in 0.2 M PB (pH 7.4) containing 0.1 M $K_2S_2O_8$ and 0.1 M KCl. Scan rate, 100 mV·s^{-1}. b ECL signal from (a) bare GCE and (b) Met-AuNC/GCE in 0.2 M PB (pH 7.4) containing 0.1 M $K_2S_2O_8$ and 0.1 M KCl generated by potential steps between 0 V and −0.7 V. c Time-dependent ECL signals of the Met-AuNC/GCE in 0.2 M PB (pH 7.4) containing 0.1 M $K_2S_2O_8$ and 0.1 M KCl. The potential was cycled between 0 and −2.0 V with a scan rate of 100 mV·s^{-1}. d ECL signals of (a) BSA-AuNC/GCE and (b) Met-AuNC/GCE in 0.2 M PB (pH 7.4) containing 0.1 M $K_2S_2O_8$ and 0.1 M KCl. The potential was cycled between 0 and −2.0 V with a scan rate of 100 mV·s^{-1}. e ECL spectrum of Met-AuNC/GCE in 0.2 M PB (pH 7.4) containing 0.1 M $K_2S_2O_8$ and 0.1 M KCl
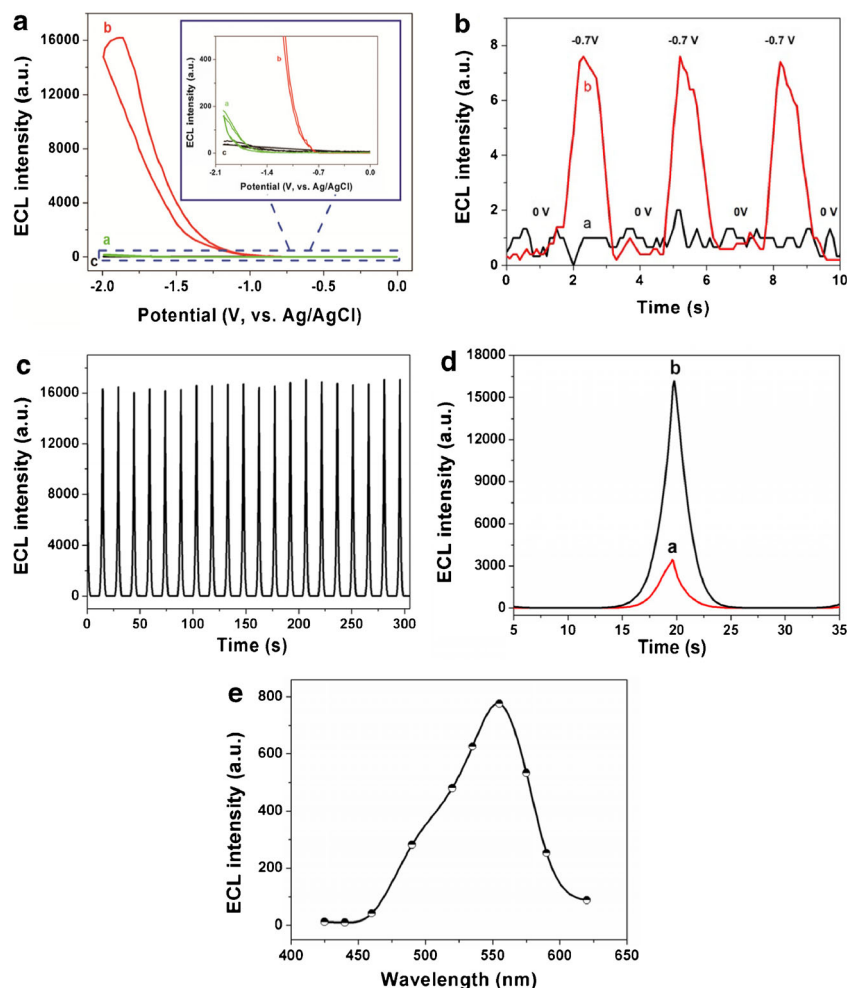
understanding of the ECL generation, we also performed the experiment in the absence of Met-AuNCs. The background ECL signal from the GCE without Met-AuNCs was very low (Fig. 2a, curve c), indicating that the ECL emission was originated from the Met-AuNCs. On the other hand, positive shift of the ECL onset potential to −0.7 V was observed on the Met-AuNC/GCE. This is further confirmed by potential step experiment. As shown in Fig. 2b, light emission was generated on Met-AuNC/GCE when the potential step from 0 V to −0.7 V, while no light emission was observed on GCE. These results suggested that Met-AuNCs accelerated electron transfer between the electrode and $S_2O_8^{2-}$ [24]. Figure 2c shows the ECL emission of Met-AuNC/GCE with 0.1 M $S_2O_8^{2-}$ under continuous cyclic voltammetry between 0 and −2.0 V of 20 cycles. Strong and stable ECL signals were observed with the relative standard deviation (RSD) of 1.9%, demonstrating that the ECL emission of Met-AuNC/GCE was high repeatable for further analytical application.

To our best knowledge, the AuNCs protected by bovine serum albumin (BSA-AuNCs) are the most frequently used AuNC-based ECL luminophore [24, 25]. Herein, we found that the ECL intensity of Met-AuNC/GCE was about five

times higher than that of BSA-AuNC/GCE (Fig. 2d, Fig. S1), suggesting that the surface ligand of AuNCs played an important role in ECL reaction. On the other hand, due to the nonconductive protein shell, the BSA-AuNCs showed much higher electron-transfer resistance (R_{et}) than that of Met-AuNCs, which resulted in the decrease of the electron transfer rate between the modified electrode and $S_2O_8^{2-}$ (Fig. S3). Thus, methionine not only acts as reducing and stabilizing reagent for the synthesis of AuNCs, but also enhances the sensitivity of ECL detection.
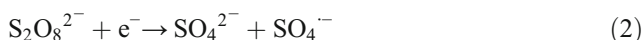
The ECL spectrum of Met-AuNCs was measured by employ in a series of optical filters. Figure 2e showed a maximum ECL emission at 550 nm with a red shift of 20 nm compared to that in the PL. This red shift between PL and ECL emission was also observed in the previously reported ECL of CdSe nanocrystals [30], Si nanocrystals [31], and peptide nanovesicles [32], which was explained to the strong role of surface states on the ECL process of the luminophore species.

All the above results implied that Met-AuNCs and $S_2O_8^{2-}$ can form an excellent ECL system (Met-AuNCs/$S_2O_8^{2-}$), in which Met-AuNCs are the luminophores while $S_2O_8^{2-}$ acts as the coreactant. The ECL emission mechanism was caused by
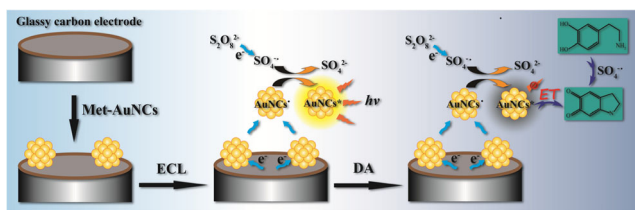
Scheme 1 Schematic diagram for the ECL sensor based on Met-AuNCs

electron transfer annihilation between an anionic quantum dot radical ($R^{\bullet-}$) and the electrogenerated $SO_4^{\bullet-}$. The possible ECL mechanism is described in Scheme 1 with the following Eqs. [10]:
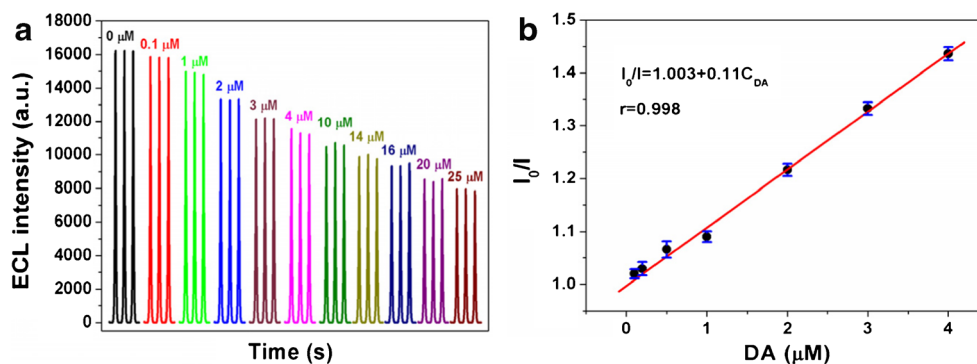
$$Met-AuNC + e^- \rightarrow Met-AuNC^{\bullet-} \tag{1}$$

$$S_2O_8^{2-} + e^- \rightarrow SO_4^{2-} + SO_4^{\bullet-} \tag{2}$$

$$Met-AuNC^{\bullet-} + SO_4^{\bullet-} \rightarrow Met-AuNC^* + SO_4^{2-} \tag{3}$$

$$Met-AuNC^* \rightarrow Met-AuNC + h\nu \tag{4}$$

Electrochemiluminescence efficiency

The ECL efficiency (Φ_{ECL}) for an annihilation system is defined as the number of photons emitted per redox event. It is the product of the efficiency of populating the excited state and the quantum yield of emission from that excited state. Eq. (5) was used to determine Φ_{ECL} of the Met-AuNCs using $[Ru(bpy)_3]^{2+}$ in the solution as a relative standard [33, 34]:

$$\Phi_{ECL} = \Phi^{\circ}_{ECL}\left(IQ^{\circ}_f/Q_f I^{\circ}\right) \tag{5}$$

where Φ°_{ECL} is the ECL efficiency of $[Ru(bpy)_3]^{2+}$ (1 mM and 0.1 M TBABF/ACN), taken as 5.0% [35], Q_f and Q°_f are the corresponding faradaic charge passed for the Met-AuNC film and $[Ru(bpy)_3]^{2+}$ respectively, and I and I° are the integrated photomultiplier tube responses for them respectively. The Φ_{ECL} of Met-AuNCs was estimated to be 2.23%, which was much higher than that of BSA-AuNCs (0.325%), Polyaniline-$[Ru(bpy)_2PIC]^{2+}$ (1.00%) [36], nafion-$[Ru(bpy)_3]^{2+}$ (0.089%) [34] and $[Ru(bpy)_2(poly-4-vinyl pyridine)_{10}]^{2+}$ (0.152%) [33].

Optimization of method

In order to improve the performance of the ECL sensor, the following parameters were optimized: (a) amount of Met-AuNCs, (b) $K_2S_2O_8$ concentration and (c) pH of the solution. Respective data and Figures are given in the Electronic Supporting Material. We found the following experimental conditions to give best results: (a) An amount of Met-AuNCs of 6.12 μg; (b) a pH of 7.4; (c) a $K_2S_2O_8$ concentration of 0.1 M (Fig. S4).

Analytical performance of the ECL sensor

DA is an important neurotransmitter of catecholamine in the human brain. The temporal fluctuation of the DA concentrations in the human brain has a critical effect on several neurological disorders such as Harrington's disease and Parkinson's disease [37–40]. The efficient determination of DA becomes increasingly significant in the field of clinical disease diagnosis and the research of physiological functions [41–53]. Thus, DA was taken as a model analyte to evaluate the potential application of the Met-AuNC-based ECL sensor. When a trace of DA was added into the detection solution, the cathodic ECL emission of Met-AuNC/GCE was quenched. The ECL intensity decreased with the increasing concentration of DA (Fig. 3a), leading to an analytical method for the detection of quenchers and quencher relatives based on the ECL of Met-AuNCs. The quenching mechanism of DA to ECL might be as follows (Scheme 1): $SO_4^{\bullet-}$, a strong radical oxidant produced by electro-reduction of $S_2O_8^{2-}$, oxidized DA to produce o-benzoquinone species. The energy transfer between Met-AuNCs excited state and o-benzoquinone species might be responsible for the quenching effect [41]. To further demonstrate the speculation, the ECL intensity of the PDA (the oxidized dopamine)/Met-AuNC-modified GCE was studied. As expected, compared with the Met-AuNC/GCE, the ECL intensity of the PDA/Met-AuNC/GCE decreased obviously (Fig. S5), which indicated that the oxidized DA can mainly lead to the ECL quenching of the Met-AuNC/GCE. With the increasing amount of DA ranging from 0.1 to 4 μM, the plot of I_0/I vs. the concentration of DA showed a

Fig. 3 **a** ECL profiles of the Met-AuNC/GCE in the presence of DA in 0.2 M PB (pH 7.4) containing 0.1 M $K_2S_2O_8$ and 0.1 M KCl. The potential was cycled between 0 and −2.0 V with a scan rate of 100 mV·s^{-1}. **b** Linear calibration plot for DA detection

good correlation (Fig. 3b), which hinted that the quenching followed the dynamic principle described by the Stern-Volmer equation,

$$I_0/I = 1 + K_{SV}[Q] \qquad (6)$$

where I_0 is the initial ECL intensity, I is the ECL intensity at a given concentration of quencher $[Q]$, and K_{SV} is the quenching constant.

Under the optimal conditions, the limit of detection was 32 nM ($S/N = 3$). The linear range and detection limit of this sensor was compared with other methods reported previously (Table 1), showing that this ECL sensor has much lower detection limit than those of some other ECL sensors [7, 24, 42, 43], electrochemistry sensors [44–49] and fluorescence sensors [50, 51]. The results presented in Table 1 indicated that the analytical performance of this sensor was better than that of the other existing sensors for detection of DA. Thus, this method not only expanded the application of Met-AuNCs, but also opened new doors toward the rapid detection of DA.

The selectivity is one of the major concerns for ECL sensors. An interference investigation was performed by using the solution containing 0.5 μM DA and 5.0 μM common co-existing substances such as uric acid (UA), ascorbic acid (AA), cysteine, glucose (Glu), glycine, lysine, citric acid, fructose, maltose, H_2O_2, CO_3^{2-}, K^+, Na^+, Mg^{2+}, Cl^-, and NO_3^-, respectively [32, 49, 54–57]. It was found that the above interfering substances do not cause a noticeable interference to the detection of DA (Fig. 4). Thus, the Met-AuNC/GCE has high selectivity for the determination of DA. The good selectivity for DA might be attributed to the efficient energy transfer between Met-AuNCs excited state and o-benzoquinone species produced by the oxidation of DA [37].
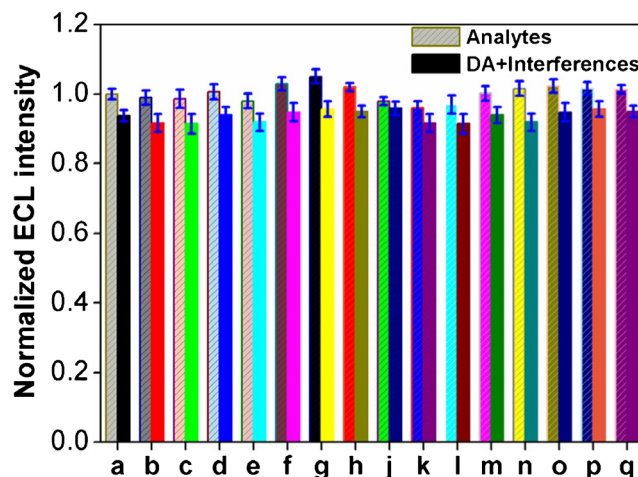

Fig. 4 Selectivity of the Met-AuNC-modified GCE/$K_2S_2O_8$ system based sensor for DA in the solution containing analytes (*left*) and 0.5 μM DA + 5 μM interferences (*right*): (*a*) blank, (*b*) UA, (*c*) AA, (*d*) cysteine, (*e*) Glu, (*f*) glycine, (*g*) lysine, (*h*) citric acid, (*i*) fructose, (*j*) maltose, (*k*) H_2O_2, (*l*) CO_3^{2-}, (*m*) K^+, (*n*) Na^+, (*o*) Mg^{2+}, (*p*) Cl^-, (*q*) NO_3^-

Detection of dopamine released by cells

Another attractive feature of this method is that it can be used for assaying the K^+-stimulated DA release from PC12 cells. To validate the practicality of the present method, three samples containing certain amounts of DA in the elevated-K^+ PB solution containing 0.1 M $K_2S_2O_8$ were prepared, and the amounts of DA in the mixtures were measured using this method. The results presented in Table S1 indicated that this approach had good accuracy in measuring K^+-stimulated DA samples that release from PC12 cells by the present method. Furthermore, Fig. 5a shows representative ECL profiles of PC12 cells that had been stimulated with K^+ ions and spiked
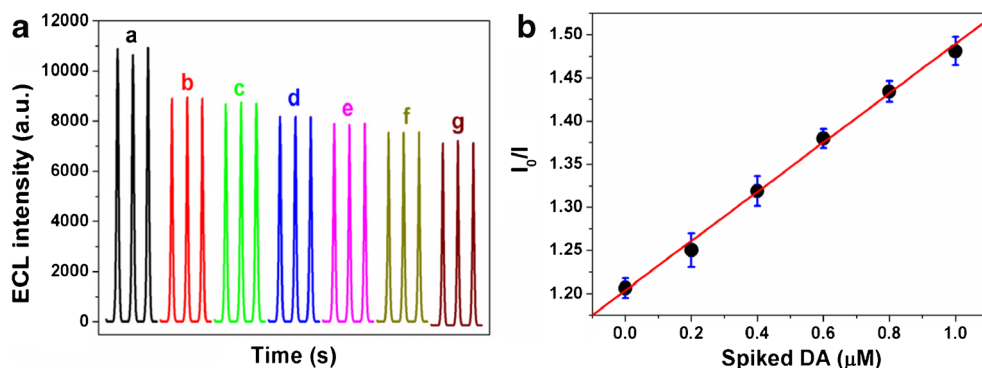
Table 1 Comparison of different methods for the detection of DA

Detection technique	Porbe	Linear range (M)	Detection limit (M)	References
ECL	rGO/MWCNs/AuNPs	2.0×10^{-7}–7.0×10^{-6}	6.7×10^{-8}	[42]
ECL	BSA-AuNC/ITO	2.5×10^{-6}–4.75×10^{-5}	2.5×10^{-6}	[24]
ECL	Ag$_2$Se quantum dot	5.0×10^{-7}–1.9×10^{-5}	1.0×10^{-7}	[7]
ECL	CdSe quantum dot	5.0×10^{-7}–7.0×10^{-5}	5.0×10^{-7}	[43]
CV[a]	Mn$_3$O$_4$ NP	1.0×10^{-6}–7.0×10^{-6}	1.0×10^{-7}	[44]
DPV[b]	erGO/ImAS/GCE	5.0×10^{-6}–2.0×10^{-4}	5×10^{-6}	[45]
DPV	PEDOT-Ni/Si	1.2×10^{-5}–4.8×10^{-5}	1.5×10^{-6}	[46]
DPV	GS-Au$_{25}$ NP	1.0×10^{-6}–1.5×10^{-5}	2.9×10^{-7}	[47]
DPV	MoS$_2$/rGO	5.0×10^{-6}–5.4×10^{-4}	5×10^{-8}	[48]
Amperometry	Pd-NC/rGO/GCE	2.0×10^{-5}–2.0×10^{-5}	7.02×10^{-6}	[49]
Fluorescence	GO	2.5×10^{-7}–2.0×10^{-5}	9.4×10^{-8}	[50]
Fluorescence	F-CuInS$_2$ quantum dot	5.0×10^{-7}–4.0×10^{-5}	2.0×10^{-7}	[51]
ECL	Met-AuNC/GCE	1.0×10^{-7}–4.0×10^{-6}	3.2×10^{-8}	This work

[a] cyclic voltammetry,

[b] differential pulse voltammetry

with standard DA solutions at various concentrations. From the linear plot, we estimated the concentration of DA released from the PC12 cells to be 0.75 μM (Fig. 5b), which is in agreement with the literature [27]. These observations substantially demonstrated that the method can be used for detection of DA in real biological samples.

Conclusions

In summary, an ECL sensor based on Met-AuNC-modified GCE has been developed. The Met-AuNCs with good water dispersibility and excellent conductivity were synthesized by using methionine both as a reductant and a stabilizer. The excellent cathodic ECL behavior of Met-AuNC/GCE has been observed with K$_2$S$_2$O$_8$ as coreactant. Fabricated with different shell ligand, the Met-AuNCs showed not only different spectroscopic characterization of the ECL (yellow color luminescence) from that of BSA-AuNCs (red color luminescence) but also significantly enhanced signal as compared to BSA-AuNCs. These phenomena prompt that AuNC-based ECL probes with tunable luminescent properties may be obtained by varying the shell ligand and have potential applications in bioanalysis such as multi-labeling techniques. In addition, the ECL system showed acceptable accuracy and precision for the detection for the model analyte DA released from PC12 cells. Therefore, this study not only enriches the foundation study about the ECL properties of AuNCs but also opens up a new avenue to design and development of ECL devices from other functional-metal based NCs. We believe that the use of the bioinspired AuNCs with excellent properties would bring huge potential in the ECL bioanalytical applications.

References

1. Yin XB, Dong SS, Wang EK (2004) Analytical applications of the electrochemiluminescence of tris (2, 2′-bipyridyl) ruthenium and its derivatives. TrAC Trends Anal Chem 23(6):432–441

2. Bertoncello P, Forster RJ (2009) Nanostructured materials for electrochemiluminescence (ECL)-based detection methods: recent advances and future perspectives. Biosens Bioelectron 24:3191–3200

3. Muzyka K (2014) Current trends in the development of the electrochemiluminescent immunosensors. Biosens Bioelectron 54:393–407

4. Vashist SK, Luong JHT (2015) Recent advances in electrochemical biosensing schemes using graphene and graphene-based nanocomposites. Carbon 84:519–550

5. Liu LL, Wang XY, Ma Q, Lin ZH, Chen SF, Li Y, LH L, HP Q, XG S (2016) Multiplex electrochemiluminescence DNA sensor for determination of hepatitis B virus and hepatitis C virus based on multicolor quantum dots and Au nanoparticles. Anal Chim Acta 916:92–101

6. Bertoncello P, Stewart AJ, Dennany L (2014) Analytical applications of nanomaterials in electrogenerated chemiluminescence. Anal Bioanal Chem 406(23):5573–5587

7. Cui R, YP G, Bao L, Zhao JY, Qi BP, Zhang ZL, Xie ZX, Pang DW (2012) Near-infrared electrogenerated chemiluminescence of ultrasmall Ag$_2$Se quantum dots for the detection of dopamine. Anal Chem 84(21):8932–8935

8. Han TQ, Yan T, Li YY, Cao W, Pang XH, Huang QJ, Wei Q (2015) Eco-friendly synthesis of electrochemiluminescent nitrogen-doped carbon quantum dots from diethylene triamine pentacetate and their application for protein detection. Carbon 91:144–152

9. Wang ZX, Zheng CL, Li QL, Ding SN (2014) Electrochemiluminescence of a nano Ag–carbon nanodot composite and its application to detect sulfide ions. Analyst 139(7):1751–1755

10. Dong YQ, Tian WR, Ren SY, Dai RP, Chi YW, Chen GN (2014) Graphene quantum dots/l-cysteine coreactant electrochemiluminescence system and its application in sensing lead (II) ions. ACS Appl Mater Interfaces 6(3):1646–1651

11. Antonello S, Perera NV, Ruzzi M, Gascon JA, Maran F (2013) Interplay of charge state, lability, and magnetism in the molecule-like Au25 (SR) 18 cluster. J Am Chem Soc 135(41):15585–15594

12. Feng JJ, Huang H, Zhou DL, Cai LY, QQ T, Wang AJ (2013) Peptide-templated synthesis of wavelength-tunable fluorescent gold nanoparticles. J Mater Chem C 31(1):4720–4725

13. Cao XL, Li HW, Lian LL, Xu N, Lou DW, YQ W (2015) A dual-responsive fluorescence method for the detection of clenbuterol based on BSA-protected gold nanoclusters. Anal Chim Acta 871:43–50

14. Negishi Y, Nobusada K, Tsukuda T (2005) Glutathione-protected gold clusters revisited: bridging the gap between gold (I)-thiolate complexes and thiolate-protected gold nanocrystals. J Am Chem Soc 127(14):5261–5270

15. ZK W, Jin RC (2010) On the ligand's role in the fluorescence of gold nanoclusters. Nano Lett 10(7):2568–2573

16. Xie J, Zheng Y, Ying JY (2009) Protein-directed synthesis of highly fluorescent gold nanoclusters. J Am Chem Soc 131(3):888–889

17. WW X, Li YD, Gao Y, Zeng XC (2016) Unraveling a generic growth pattern in structure evolution of thiolate-protected gold nanoclusters. Nanoscale 8:7396–7401

18. Wen F, Dong YH, Feng L, Wang S, Zhang S, Zhang XR (2011) Horseradish peroxidase functionalized fluorescent gold nanoclusters for hydrogen peroxide sensing. Anal Chem 83(4):1193–1196

19. Liu CL, HT W, Hsiao YH, Lai CW, Shih CW, Peng YK, Tang KC, Chang HW, Chien YC, Hsiao JK, Cheng JT, Chou PT (2011) Insulin-directed synthesis of fluorescent gold nanoclusters: preservation of insulin bioactivity and versatility in cell imaging. Angew Chem Int Ed 50(31):7056–7060

20. Nair LV, Philips DS, Jayasree RS, Ajayaghosh AA (2013) A near-infrared fluorescent nanosensor (AuC@urease) for the selective detection of blood urea. Small 9(16):2673–2677

21. XY M, Li Q, Dong P, Qiao J, Hou J, Nie ZX, Ma HM (2013) Facile one-pot synthesis of L-proline-stabilized fluorescent gold nanoclusters and its application as sensing probes for serum iron. Biosens Bioelectron 49:249–255

22. Deng HH, GW W, Zou ZQ, Peng HP, Liu AL, Lin XH, Xia XH, Chen W (2015) pH-sensitive gold nanoclusters: preparation and analytical applications for urea, urease, and urease inhibitor detection. Chem Commun 51:7847–7850

23. Wang CX, Wang Y, Xu L, Shi XD, Li XW, XW X, Sun HC, Yang B, Lin Q (2013) A galvanic replacement route to prepare strongly fluorescent and highly stable gold nanodots for cellular imaging. Small 9(3):413–420

24. Li LL, Liu HY, Shen YY, Zhang JR, Zhu JJ (2011) Electrogenerated chemiluminescence of Au nanoclusters for the detection of dopamine. Anal Chem 83(3):661–665

25. Fang YM, Song J, Li J, Wang YW, Yang HH, Sun JJ, Chen GN (2011) Electrogenerated chemiluminescence from Au nanoclusters. Chem Commun 47:2369–2371

26. Deng HH, Zhang LN, He SB, Liu AL, Li GW, Lin XH, Xia XH, Chen W (2015) Methionine-directed fabrication of gold nanoclusters with yellow fluorescent emission for Cu^{2+} sensing. Biosens Bioelectron 65:397–403

27. Tsai HY, Lin ZH, Chang HT (2012) Tellurium-nanowire-coated glassy carbon electrodes for selective and sensitive detection of dopamine. Biosens Bioelectron 35:479–483

28. Wang C, Hu YJ, Lieber CM, Sun SH (2008) Ultrathin Au nanowires and their transport properties. J Am Chem Soc 130(28):8902–8903

29. Jie GF, Zhang JJ, Wang DC, Cheng C, Chen HY, Zhu JJ (2008) Electrochemiluminescence immunosensor based on CdSe nanocomposites. Anal Chem 80(11):4033–4039

30. Myung N, Ding ZF, Bard AJ (2002) Electrogenerated chemiluminescence of CdSe nanocrystals. Nano Lett 2(11):1315–1319

31. Ding ZF, Quinn BM, Haram SK, Pell LE, Korgel BA, Bard AJ (2002) Electrochemistry and electrogenerated chemiluminescence from silicon nanocrystal quantum dots. Science 296(5571):1293–1297

32. Huang CX, Chen X, YL L, Yang H, Yang WS (2015) Electrogenerated chemiluminescence behavior of peptide nanovesicle and its application in sensing dopamine. Biosens Bioelectron 63:478–482

33. O'Reilly EJ, Keyes TE, Forster RJ, Dennany L (2012) Insights into electrochemiluminescent enhancement through electrode surface modification. Analyst 138:677–682

34. Dennany L, Hogan C, Keyes T, Forster RJ (2006) Effect of surface immobilization on the electrochemiluminescence of ruthenium-containing metallopolymers. Anal Chem 78(5):1412–1417

35. Wallace WL, Bard AJ (1979) Electrogenerated chemiluminescence. 35. Temperature dependence of the ECL efficiency of tris(2,2′-bipyridine)rubidium(2+) in acetonitrile and evidence for very high excited state yields from electron transfer reactions. J Phys Chem 83(10):1350–1357

36. Molapo KM, Venkatanarayanan A, Dolan CM, Prendergast U, Baker PG, Iwuoha EI, Keyes TE, Forster R (2014) High efficiency electrochemiluminescence from polyaniline: ruthenium metal complex films. Electrochem Commun 48:95–98

37. Clarke SJ, Hollmann CA, Zhang Z, Suffern D, Bradforth SE, Dimitrijevic NM, Minarik WG, Nadeau JL (2006) Photophysics of dopamine-modified quantum dots and effects on biological systems. Nat Mater 5:409–417

38. Yusoff N, Pandikumar A, Ramaraj R, Ngee LH, Huang NM (2015) Gold nanoparticle based optical and electrochemical sensing of dopamine. Microchim Acta 182:2091–2114

39. Sanghavi BJ, Wolfbeis OS, Hirsch T, Swami NS (2015) Nanomaterial-based electrochemical sensing of neurological drugs and neurotransmitters. Microchim Acta 182:1–41

40. Ming L, Peng T, Tu Y (2016) Multiple enhancement of luminol electrochemiluminescence using electrodes functionalized with titania nanotubes and platinum black: ultrasensitive determination of hydrogen peroxide, resveratrol, and dopamine. Microchim Acta 183:305–310

41. Liu X, Jiang H, Lei JP, HX J (2007) Anodic electrochemiluminescence of CdTe quantum dots and its energy transfer for detection of catechol derivatives. Anal Chem 79:8055–8060

42. Yuan DH, Chen SH, Yuan R, Zhang JJ, Liu XF (2014) An ECL sensor for dopamine using reduced graphene oxide/multiwall carbon nanotubes/gold nanoparticles. Sensors Actuators B Chem 191:415–420

43. Liu X, Cheng L, Lei J, Ju H (2008) Dopamine detection based on its quenching effect on the anodic electrochemiluminescence of CdSe quantum dots. Analyst 133(9):1161–1163

44. Gao WW, Ye SY, Shao MW (2011) Solution-combusting preparation of mono-dispersed Mn_3O_4 nanoparticles for electrochemical applications. J Phys Chem Solids 72(9):1027–1031

45. Wu F, Huang T, Hu Y, Yang X, Ouyang Y, Xie Q (2016) Differential pulse voltammetric simultaneous determination of ascorbic acid, dopamine and uric acid on a glassy carbon electrode modified with electroreduced graphene oxide and imidazolium groups. Microchim Acta 183(9):2539–2546

46. SJ Y, Luo CH, Wang LW, Peng H, Zhu ZQ (2013) Poly(3, 4-ethylenedioxythiophene)-modified Ni/silicon microchannel plate electrode for the simultaneous determination of ascorbic acid, dopamine and uric acid. Analyst 138(4):1149–1155

47. Kwak K, Kumar SS, Lee D (2012) Selective determination of dopamine using quantum-sized gold nanoparticles protected with charge selective ligands. Nanoscale 4(14):4240–4246

48. Xing L, Ma Z (2016) A glassy carbon electrode modified with a nanocomposite consisting of MoS_2 and reduced graphene oxide for electrochemical simultaneous determination of ascorbic acid, dopamine, and uric acid. Microchim Acta 183(1):257–263

49. Hsieh YS, Hong BD, Lee CL (2016) Non-enzymatic sensing of dopamine using a glassy carbon electrode modified with a nanocomposite consisting of palladium nanocubes supported on reduced graphene oxide in a nafion matrix. Microchim Acta 183(2):905–910

50. Chen JL, Yan XP, Meng K, Wang SF (2011) Graphene oxide based photoinduced charge transfer label-free near-infrared fluorescent biosensor for dopamine. Anal Chem 83(22):8787–8793

51. Liu S, Shi F, Zhao X, Chen L, Su X (2013) 3-Aminophenyl boronic acid-functionalized $CuInS_2$ quantum dots as a near-infrared fluorescence probe for the determination of dopamine. Biosens Bioelectron 47:379–384

52. Wang T, Zhang SY, Mao CJ, Song JM, Niu HL, Jin BK, Tian YP (2012) Enhanced electrochemiluminescence of CdSe quantum dots composited with graphene oxide and chitosan for sensitive sensor. Biosens Bioelectron 31:369–375

53. Jin L, Gao X, Wang L, Wu Q, Chen Z, Lin X (2013) Electrochemical activation of polyethyleneimine-wrapped carbon nanotubes/in situ formed gold nanoparticles functionalised nano-composite sensor for high sensitive and selective determination of dopamine. J Electroanal Chem 692:1–8

54. Liu SF, Zhang X, YM Y, Zou GZ (2014) A monochromatic electrochemiluminescence sensing strategy for dopamine with dual-stabilizers-capped CdSe quantum dots as emitters. Anal Chem 86:2784–2788

55. Li JX, Li XJ, Zhang YH, Li RX, Wu D, Du B, Zhang Y, Ma HM, Wei Q (2015) Electrochemiluminescence sensor based on cationic polythiophene derivative and NH_2–graphene for dopamine detection. RSC Adv 5:5432–5437

56. Rao D, Zhang X, Sheng Q, Zheng J (2016) Highly improved sensing of dopamine by using glassy carbon electrode modified with MnO_2, graphene oxide, carbon nanotubes and gold nanoparticles. Microchim Acta 83(9):2597–2604

57. Mei LP, Feng JJ, Wu L, Chen JR, Shen L, Xie Y, Wang AJ (2016) A glassy carbon electrode modified with porous Cu_2O nanospheres on reduced graphene oxide support for simultaneous sensing of uric acid and dopamine with high selectivity over ascorbic acid. Microchim Acta 183(6):2039–2046